Real-time simulations of photoinduced coherent charge transfer and proton-coupled electron transfer

Eisenmayer, T.J.; Buda, F.

ChemPubSoc Europe

DOI: 10.1002/cphc.201402444

Real-time Simulations of Photoinduced Coherent Charge Transfer and Proton-Coupled Electron Transfer

Thomas J. Eisenmayer and Francesco Buda*[a]

Photoinduced electron transfer (ET) and proton-coupled electron transfer (PCET) are fundamental processes in natural phenomena, most noticeably in photosynthesis. Time-resolved spectroscopic evidence of coherent oscillatory behavior associated with these processes has been reported both in complex biological environments, as well as in biomimetic models for artificial photosynthesis. Here, we consider a few biomimetic models to investigate these processes in real-time simulations based on ab initio molecular dynamics and Ehrenfest dynamics. This allows for a detailed analysis on how photon-to-charge conversion is promoted by a coupling of the electronic excitation with specific vibrational modes and with proton displacements. The ET process shows a characteristic coherence that is linked to the nuclear motion at the interface between donor and acceptor. We also show real-time evidence of PCET in a benzimidazole–phenol redox relay.

1. Introduction

Electron transfer (ET) and proton-coupled electron transfer (PCET) are fundamental processes in many biochemical reactions and molecular electronic device functions.[1–3] This is particularly evident in natural photosynthesis, where photoinduced charge separation is the first fundamental step leading to the conversion of solar energy into chemical energy.[4,5] Also, in the oxygen-evolving complex (OEC) of Photosystem II (PSII), successive PCET reaction steps are crucially important to overcome the thermodynamically demanding water-splitting reaction, avoiding the accumulation of excess positive charge in the manganese cluster.[6] Moreover in PSII, a tyrosine–histidine pair, which mediates the ET between the OEC and the radical cation $P680^+$, provides a kinetic control between the slow catalytic water-oxidation steps and the fast photoinduced charge transfer through an intermolecular PCET process.[7,8]

There is growing experimental and theoretical evidence of oscillatory features associated with the energy and electron transfer in natural and artificial photosynthetic complexes.[9–12] Understanding the nature and the role of this coherent dynamics is important both from a fundamental and technological point of view, as it may provide hints for the design of molecular devices for solar to fuel conversion.[4,13]

Photoinduced ET processes are usually analyzed in the context of Marcus theory. However, the validity of this approach for fast ET or PCET processes in supramolecular complexes is often under scrutiny. Here, we use instead Ehrenfest dynamics simulations to overcome this issue and investigate in real time the coupling between the electronic motion and specific vibrational modes of the complex. In particular, we consider a donor–acceptor hydrogen-bonded complex formed by melamine (1,3,5-triazine-2,4,6-triamine) and isocyanuric acid (1,3,5-triazine-2,4,6-trione) mimicking DNA base pairing. We also present ab initio molecular dynamics simulations of the benzimidazole–phenol redox relay recently included in an artificial triad for efficient charge separation[8] and show real-time evidence of the PCET process leading to the formation of the stable phenoxyl radical.

[a] T. J. Eisenmayer, Dr. F. Buda
Leiden Institute of Chemistry, Leiden University
Einsteinweg 55, 2300 RA Leiden (The Netherlands)
E-mail: f.buda@chem.leidenuniv.nl

Supporting Information for this article is available on the WWW under http://dx.doi.org/10.1002/cphc.201402444.

Models and Methods

Photoinduced ET

For time-dependent Kohn–Sham (TDDFT) simulations of photoinduced ET, we consider a supramolecular complex consisting of melamine and isocyanuric acid held together by a hydrogen-bonding network (Scheme 1).[14] The biomimicry of the model lies in its resemblance with DNA base pairing as it self-assembles into a tile-like structure with two-dimensional hydrogen bonds.[15]

The geometry optimization of the complex is performed with the ADF program[16] at the BLYP/TZP level of theory. The optimized geometry is then used to perform a spin-polarized single-point LDA[17] density optimization on a real space grid with 52 Ry cutoff by using the OCTOPUS suite.[18–21] The core electrons are described

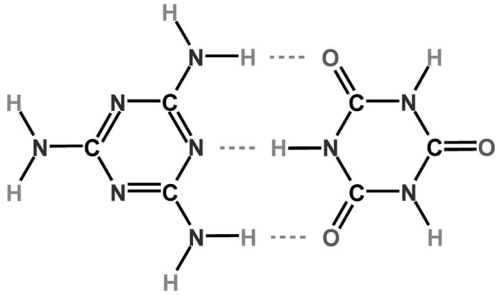

Scheme 1. Melamine (donor; left) and isocyanuric acid (acceptor; right).

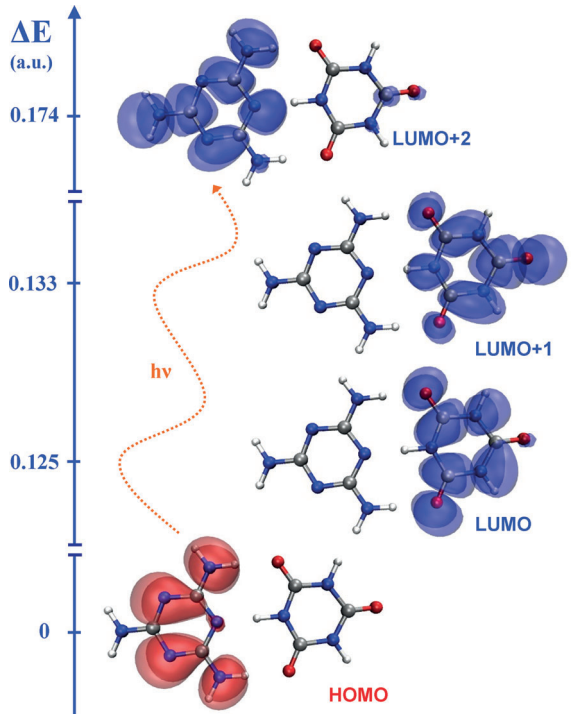

Figure 1. Localization of the frontier molecular orbitals. The photoexcitation {HOMO}→{LUMO+2} and its energy are shown together with the gradients for photoinduced charge transfer {LUMO+2}→{LUMO+1/LUMO}.

by Troullier–Martins pseudopotentials in SIESTA format.[22] From the obtained set of occupied and unoccupied states we prepare the system in a single-particle excited state on the melamine, by depopulating the HOMO and populating the LUMO+2 (Figure 1). By means of linear-response TDDFT (ADF, LDA/TZP) we verify that these orbitals contribute most to the dominant optical transition. We have performed additional test calculations with different hybrid and long-range corrected functionals and a reference high-level ab initio method to check the effect on the relevant orbital and excitation energies (see the Supporting Information). These tests confirm that the orbital energies are almost unaffected by the choice of the specific exchange-correlation functional and that the exciton state is consistently higher in energy than the charge-transfer state. Subsequently we solve the TDDFT equations by using the OCTOPUS quantum-chemical suite[18–21] with a time step of 2 as. To approximate the evolution operator we use the approximated enforced time-reversal symmetry (AETRS) algorithm[21] and the exponential of the Hamiltonian is calculated by Taylor expansion. The nuclei are propagated classically within the Ehrenfest formalism.[23] To quantify the photoinduced ET along the dynamics we monitor the photoinduced spin density (PSD) [Eq. (1)]:

$$\mathrm{PSD}(r) = \rho^{\beta}(r) - \rho^{\alpha}(r) = \sum_{i}^{N/2} \left|\phi_i^{\beta}(r)\right|^2 - \sum_{i}^{N/2} \left|\phi_i^{\alpha}(r)\right|^2 \quad (1)$$

where ρ represents the density, α and β the respective spin species, N the number of electrons, and ϕ_i the Kohn–Sham molecular orbitals. Although the total spin of the system is equal to 0, the spatial spin distribution upon photoexcitation will show regions with an excess of α or β spin. By partitioning the simulation box in two halves, one containing the electron donor (melamine) and the other containing the electron acceptor (isocyanuric acid) we quantify the amount of PSD transferred through the hydrogen-bond network. Furthermore, the negative/depleted regions of the PSD give the spatial localization of the photoinduced hole, whereas regions with an increase in PSD correspond to the photoinduced ET.

PCET

We present real-time simulations of PCET on a single adiabatic potential energy surface. The model we study is a benzimidazole–phenol (Scheme 2) that mimics the tyrosine–histidine pair in PSII.[8] In analogy with natural photosynthesis the PCET from the phenol to the benzimidazole can prevent charge recombination by stabilizing the photoinduced hole.

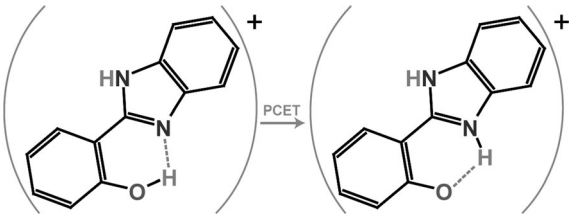

Scheme 2. PCET in benzimidazole–phenol upon (photoinduced) oxidation.

To simulate the PCET process in real time we use the Car–Parrinello method as implemented in the CPMD code.[24,25] The total time of the trajectories is 5 ps with a time step of 0.1 fs. A Nosé thermostat is used in all simulations to keep the temperature around an average of 300 K. At this temperature we expect that quantum effects on the proton dynamics are not dominant and that the classical description of the nuclear motion is appropriate. The BLYP functional[26,27] is used for the exchange-correlation energy. The Kohn–Sham orbitals are expanded in a plane-wave basis set with an energy cutoff of 70 Ry. We employ dispersion-corrected atom-centered (DCACP) pseudopotentials.[28,29] Starting from a partially optimized structure with the proton on the phenol (Scheme 2), we follow the dynamics of the proton and the unpaired electron in real time. The unpaired electron is tracked along the trajectories by monitoring the hole spin density (HSD) [Eq. (2)]:

$$\mathrm{HSD}(r) = \rho^{\beta}(r) - \rho^{\alpha}(r) \quad (2)$$

where ρ represents the density, α and β the respective spin species. The total integral over space of the HSD equals 1. By integrating the HSD over different partitions of the simulation box, representing either the phenolic moiety or the benzimidazole, we quantify the localization of the unpaired electron. We perform CPMD simulations both in vacuum and in the presence of an explicit water solvent.

2. Results and Discussion

2.1. Photoinduced ET

To follow the photoinduced ET through a hydrogen-bond network we prepare the melamine cyanurate complex in a singlet excited state on the melamine. This represents a typical exciton state, where the electron and hole are both localized on the same moiety with no net charge transfer. In terms of the photoinduced spin, we can compare the initial state of the quantum-classical dynamics (Figure 2, top left) with the in-

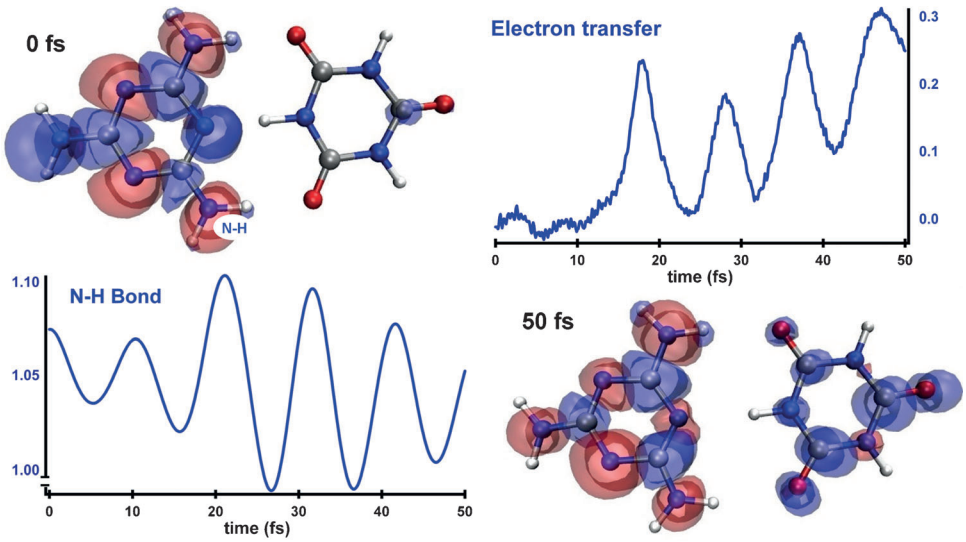

Figure 2. Coherent photoinduced ET (upper right panel) in a DNA-base-pair mimic held together by hydrogen bonds (see the Supporting Information, Movie 1). The calculations were performed in real time within the Ehrenfest formalism starting from the localized PSD in the upper left panel. The PSD after 50 fs (lower right panel) shows ET (blue) to the isocyanuric acid and an accumulation of the hole (red) on the melamine. The fluctuations in the hydrogen-bond network, illustrated by the N–H bond (Å) in the lower left panel, indicate a coherent coupling between proton displacements and ET.

volved orbitals (Figure 1) and verify that the depleted (red) density corresponds to the HOMO and the increase (blue) corresponds to the LUMO+2. Starting from the localized exciton state on the melamine the quantum-classical dynamics simulation shows charge transfer through the hydrogen-bond network with superimposed temporal oscillations with a period of approximately 10 fs (Figure 2, upper right panel). In wavenumbers this equals $\approx$3300 cm^{-1}, which lies in the amine N–H stretching mode range, thus suggesting a coherent coupling of the (nonadiabatic) ET with nuclear motion involving the hydrogen-bond network. This is further illustrated by simply comparing the N–H bond dynamics (Figure 2, bottom left panel) with the oscillatory ET along the trajectory, both exhibiting the same number of oscillations within the simulation time. The total charge transferred in 50 fs amounts to $\approx$0.3 electron equivalents. Movie 1, in the Supporting Information, shows the PSD along the dynamics, where this oscillatory behavior in the charge transfer is evident. Longer simulations do not show a further increase in the photoinduced charge transfer through the hydrogen-bonding network.

In photosynthesis, coherent charge and energy transfer has been observed at ambient temperature in complex biological surroundings.[9–11] The near unity quantum yield of photon-to-charge conversion in photosynthetic complexes stems from such concerted nuclear motion of the chromophore and a responsive protein matrix.[4,11] The responsiveness lies in the fact that the matrix couples specific vibrations to the photoexcited chromophore that remove the barrier for photoinduced charge separation,[9,10,30,31] much like the promoting vibrations observed in enzyme catalysis.[32] Also proton displacements play an important role in facilitating ET and preventing charge recombination in photosynthetic charge separation.[31] The coherent coupling between amine stretching vibrations and photoinduced ET in melamine cyanurate (Figure 2) illustrate how proton displacements control the charge transfer in a hydrogen-bonded complex. It has recently been shown, with similar TDDFT/LDA simulations, that correlated, coherent motion of ions and electrons drives the first steps of photoinduced ET in an artificial reaction center.[12] We show that even photoexcitation of a DNA-base-pair mimic leads to such coherent motion. Based on these results, we conclude that such characteristic vibrations involve the nuclear motion at the interface between donor and acceptor. It is tempting to suggest that this oscillatory behavior is common to photoinduced charge-transfer processes. A broader investigation on a range of supramolecular complexes is needed to verify the generality and role of this phenomenon. At the same time, these coherences can be optimized to increase the efficiency of photon-to-charge conversion in molecular devices.

2.2. PCET

In many natural processes and most noticeably in photosynthesis ET is often accompanied by a concerted proton motion that reduces the probability of charge recombination. Moreover the tyrosine–histidine redox mediator in PSII becomes an extremely long-lived neutral radical after removing the hole from the special pair. As such it facilitates the kinetically demanding water oxidation in the OEC.[7]

To simulate PCET in the benzimidazole–phenol mimic of this redox mediator, we perform ab initio molecular dynamics simulations in the state after electron injection to an acceptor. In this configuration the proton is still attached to the phenol oxygen. After 180 fs of dynamical evolution we observe a first attempt of a proton transfer to the imidazole nitrogen atom (Figure 3, upper left panel; $\approx$0.2 ps). This unsuccessful approach is at the end of the first characteristic fluctuation of the hydrogen bond. After another full period of this oscillation the proton is transferred to the imidazole nitrogen atom ($\approx$0.5 ps). The proton remains stable in this configuration during the entire simulation (5 ps) even though we still observe hydrogen-bond dynamics that moves the proton close (1.3 Å) to the phenoxyl oxygen radical (see upper left panel; $\approx$0.8 ps). Initially the hole spin density is delocalized over the entire complex (Figure 3, lower left panel). After the proton transfer (0.6 ps) the spin density localizes on the phenol with a modified nodal structure forming a phenoxyl neutral radical (Figure 3, upper right panel).

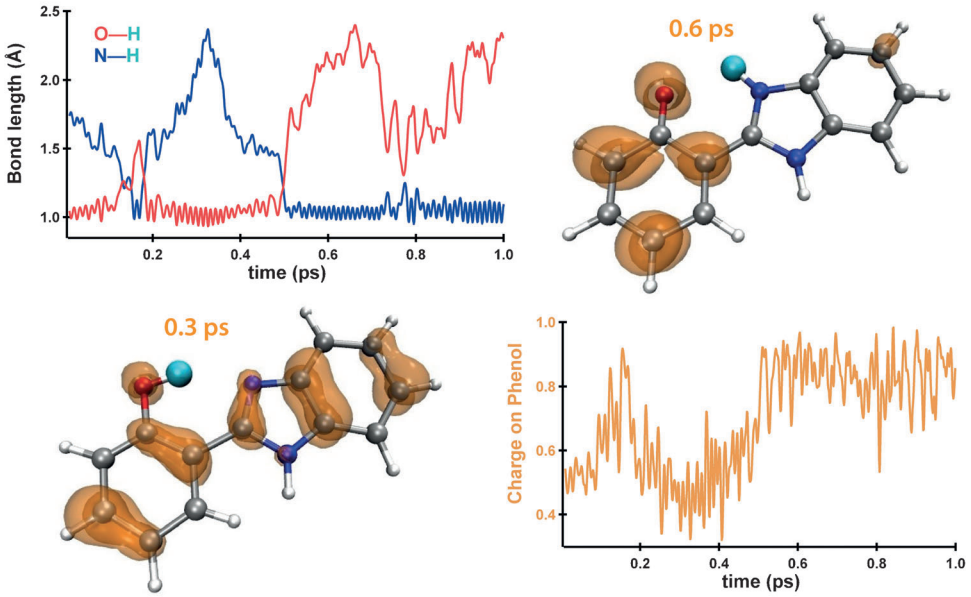

Figure 3. Real-time simulation of PCET in a mimic of the tyrosine–histidine pair in PSII (see the Supporting Information, Movie 2). We start the ab initio molecular dynamics in the configuration of the benzimidazole–phenol just after an electron has been injected into an acceptor. The upper left panel tracks the distance of the proton with respect to the phenol (O) and imidazole (N). We observe the proton transfer after approximately 0.5 ps. The hole spin density (orange) almost entirely localizes on the phenol as the proton is transferred under formation of a phenoxyl neutral radical (upper right panel). The symmetry of the unpaired electron changes with a modified nodal structure (compare lower left and upper right panels). When integrating the charge on the phenol as the simulation proceeds (lower right panel) the spin density on the phenol follows the proton motion and approximates unity after the proton transfer.

Movie 2, in the Supporting Information, illustrates the immediacy of the spin density localization upon proton transfer. The integrated spin density on the phenol ring in the lower right panel of Figure 3 quantifies the charge transfer along the dynamics. Clearly, the spin density rearranges in a concerted fashion with the proton dynamics (Figure 3, upper left panel) and approaches unity as the proton is transferred to the imidazole nitrogen atom. To investigate the possibility of a solvent-mediated proton transfer in benzimidazole–phenol we perform ab initio molecular dynamics with an explicit water solvation shell and periodic boundary conditions. We start from the same initial conditions of the redox mediator as in the vacuum simulations and evolve the system starting with the proton attached to the phenolic oxygen. The proton transfer occurs on a significantly longer time scale with the inclusion of an explicit solvent (see Figure 4). Moreover the thermal fluctuations of the intramolecular hydrogen bond are damped by the formation of hydrogen bonds with the solvent. As we established in the simulation for the isolated system, the fluctuations of the intermolecular hydrogen bond are crucial in facilitating proton transfer. The reduced amplitude of these fluctuations in the presence of solvent decreases the probability for the proton to be transferred to the imidazole. Water-assisted proton transfer through the temporary formation of a hydronium ion is not observed. In terms of hole spin density, the symmetry before and after proton transfer changes in the same fashion as in a vacuum. The nodal structure is modified and the localization is now almost entirely on the phenol, which becomes a neutral phenoxyl radical (Figure 4, bottom panels). Small fractions of spin density are also observed on water molecules, further indicating the hydrogen-bonding interaction with the solvent. We observe that the out-of-plane motion between the imidazole and phenol moieties is limited to a range of a few degrees (+5, −5), owing to the presence of an intramolecular hydrogen bond and consistent with experimental findings.[8] We find that the fluctuations in this dihedral angle are coupled to proton transfer, as they are associated with fluctuations in the distance between the proton donor and proton acceptor.

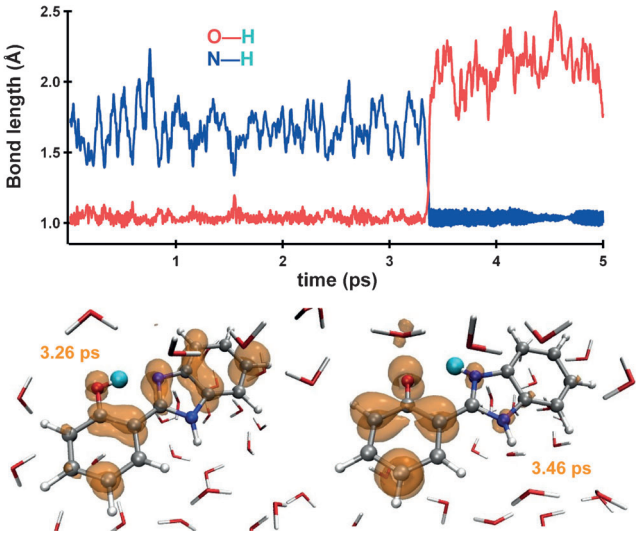

Figure 4. PCET simulation with water as the explicit solvent. We find almost an order of magnitude slower proton transfer with respect to the simulations in vacuum (upper panel), which we attribute to hydrogen bonding between the proton and the solvent. The delocalized hole spin density before proton transfer (lower left panel) localizes on the phenol after proton transfer (lower right panel) and a phenoxyl neutral radical is formed.

2.3. Artificial Reaction Center

The concept and realization of an artificial reaction center for stable photoinduced charge separation based on properly chosen molecular building blocks has been developed for many years.[5] It is generally accepted that such supramolecular complexes should comprise at least three components (triad) with a light-sensitive antenna molecule coupled to a donor and an acceptor to reach a charge-separated state that lives long enough to support the kinetically demanding redox catalytic steps. One of the most studied triads in the literature is the carotenoid–porphyrin–fullerene complex,[33] where ultrafast charge-transfer dynamics have been observed with femtosecond spectroscopy.[12] Following a similar strategy as in Reference [8], we explore a triad including a fullerene acceptor, a naphthalene diimide (NDI) antenna, and the benzimidazole–phenol (BiP) moiety discussed in the previous section as electron donor (see Figure 5).

The NDI antenna is very versatile, because it can be functionalized with different groups to adjust its optical and electronic properties.[34,35] This allows us to control the molecular-absorption range and to adapt the molecular redox properties to specific interface requirements. The BiP relay module is included in the triad to stabilize the charge-separated state through the formation of the phenoxyl radical. We have verified that this radical state is accessible in the triad upon charge separation (see Figure 5, top). We are planning to perform long real-time Ehrenfest dynamics simulations of the triad starting from the exciton state to follow the full electron/hole transfer and the PCET step leading to long-lived charge separation. These simulations should also allow us to establish whether coherent motion might play a role in this supramolecular complex, similarly to what has been observed in the carotenoid–porphyrin–C_{60} complex.[12]

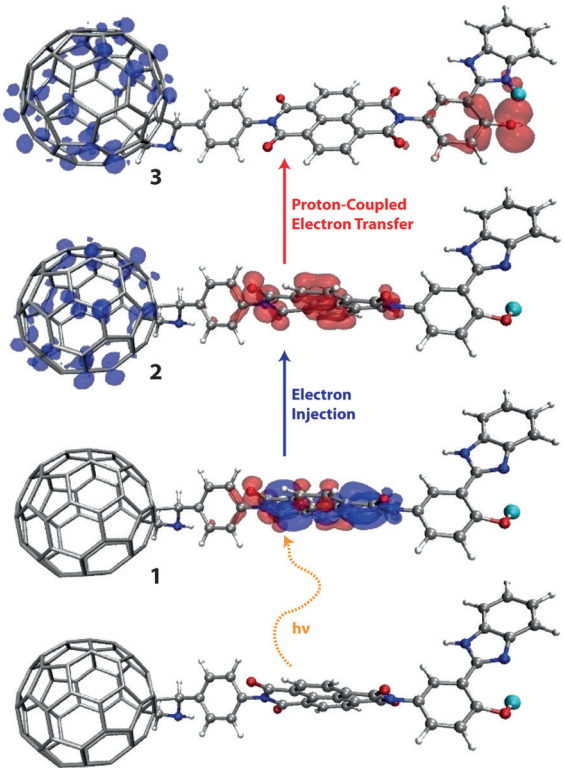

Figure 5. Artificial photosynthetic assembly consisting of a fullerene acceptor, a naphthalene diimide antenna and a benzimidazole–phenol electron donor. The latter is thought to prevent charge recombination by filling the hole on the antenna that is formed after electron injection into the acceptor. Once oxidized, the donor will transfer a proton from the phenolic moiety to the imidazole and localize the unpaired electron almost entirely on the phenol in a concerted PCET step. Depicted are the photoinduced spin densities (blue = electron, red = hole) after short TDDFT trajectories in the exciton state (**1**), the intermediate charge-transfer state (**2**), and the fully charge separated state (**3**) where the proton has been transferred to the imidazole.

3. Conclusions

We have presented ab initio molecular-dynamics and Ehrenfest dynamics simulations describing in real-time ET and PCET processes in simple molecular complexes. The photoinduced ET dynamics in a DNA-base-pair mimic interestingly showed an oscillatory behavior, which can be rationalized in terms of a strong coupling between the electronic motion and high frequency vibrational modes associated with hydrogen-bonding interactions. The dynamics in a mimic of the tyrosine–histidine pair in PSII showed proton transfer from the phenolic oxygen atom to the imidazole nitrogen atom upon oxidation. The proton dynamics is strongly coupled to the hole spin density, which localizes on the phenol leading to the formation of the phenoxyl radical. The currently available efficient implementation of Ehrenfest dynamics paves the way for extensive real-time simulations of ET and PCET processes in supramolecular complexes that can lead to in silico design of modules for artificial photosynthesis applications.

Acknowledgements

The use of supercomputer facilities was sponsored by NWO Physical Sciences, with financial support from the Netherlands Organization for Scientific Research (NWO). We acknowledge the use of the PRACE-3IP project (FP7 RI-312763) resources at ICM (IBM Power 7 based in Poland). This project was in part carried out within the research programme of BioSolar Cells, co-financed by the Dutch Ministry of Economic Affairs (project C1.9). We also acknowledge financial support from the NWO-ECHO project number 713.011.002.

Keywords: coherence · Ehrenfest dynamics · electron transfer · molecular dynamics · proton-coupled electron transfer

[1] S. Hammes-Schiffer, A. V. Soudackov, *J. Phys. Chem. B* **2008**, *112*, 14108–14123.
[2] S. Hammes-Schiffer, *Acc. Chem. Res.* **2009**, *42*, 1881–1889.
[3] C. Ko, S. Hammes-Schiffer, *J. Phys. Chem. Lett.* **2013**, *4*, 2540–2545.
[4] G. D. Scholes, G. R. Fleming, A. Olaya-Castro, R. van Grondelle, *Nat. Chem.* **2011**, *3*, 763–774.
[5] D. Gust, T. A. Moore, A. L. Moore, *Acc. Chem. Res.* **2009**, *42*, 1890
[6] H. Dau, C. Limberg, T. Reier, M. Risch, S. Roggan, P. Strasser, *ChemCatChem* **2010**, *2*, 724–761.

[7] L. Hammarström, S. Styring, *Energy Environ. Sci.* **2011**, *4*, 2379 – 2388.
[8] J. D. Megiatto Jr, D. D. Méndez-Hernández, M. E. Tejeda-Ferrari, A. Teillout, M. J. Llansola-Portolés, G. Kodis, O. G. Poluektov, T. Rajh, V. Mujica, T. L. Groy, D. Gust, T. A. Moore, A. L. Moore, *Nat. Chem.* **2014**, *6*, 423 – 428.
[9] G. S. Engel, T. R. Calhoun, E. L. Read, T. K. Ahn, T. Mančal, Y. C. Cheng, R. E. Blankenship, G. R. Fleming, *Nature* **2007**, *446*, 782.
[10] V. Novoderezhkin, A. Yakovlev, R. van Grondelle, V. Shuvalov, *J. Phys. Chem. B* **2004**, *108*, 7445.
[11] A. W. Chin, J. Prior, R. Rosenbach, F. Caycedo-Soler, S. F. Huelga, M. B. Plenio, *Nat. Phys.* **2013**, *9*, 113 – 118.
[12] C. A. Rozzi, S. M. Falke, N. Spallanzani, A. Rubio, E. Molinari, D. Brida, M. Maiuri, G. Cerullo, H. Schramm, J. Christoffers, C. Lienau, *Nat. Commun.* **2013**, *4*, 1602.
[13] E. J. Kolli, D. O'Reilly, G. Scholes, A. Olaya-Castro, *J. Chem. Phys.* **2012**, *137*, 174109.
[14] Analysis of charge-transfer effects in molecular complexes based on absolutely localized molecular orbitals: R. Z. Khaliullin, A. T. Bell, M. Head-Gordon, *J. Chem. Phys.* **2008**, *128*, 184112.
[15] L. M. Perdigão, N. R. Champness, P. H. Beton, *Chem. Commun.* **2006**, 538 – 540.
[16] ADF2012, SCM, Theoretical Chemistry, Vrije Universiteit, Amsterdam, The Netherlands, http://www.scm.com/.
[17] J. P. Perdew, A. Zunger, *Phys. Rev. B* **1981**, *23*, 5048.
[18] X. Andrade, J. Alberdi-Rodriguez, D. A. Strubbe, M. J. T. Oliveira, F. Nogueira, A. Castro, J. Muguerza, A. Arruabarrena, S. G. Louie, A. Aspuru-Guzik, A. Rubio, M. A. L. Marques, *J. Phys. Condens. Matter* **2012**, *24*, 233202.
[19] H. Castro, M. O. Appel, C. A. Rozzi, X. Andrade, F. Lorenzen, M. A. L. Marques, E. K. U. Gross, A. Rubio, *Phys. Status Solidi B* **2006**, *243*, 2465 – 2488.
[20] M. A. L. Marques, A. Castro, G. F. Bertsch, A. Rubio, *Comput. Phys. Commun.* **2003**, *151*, 60 – 78.
[21] A. Castro, M. A. L. Marques, A. Rubio, *J. Chem. Phys.* **2004**, *121*, 3425 – 3433.
[22] N. Troullier, J. L. Martins, *Phys. Rev. B* **1991**, *43*, 1993 – 2006.
[23] X. Andrade, A. Castro, D. Zueco, J. L. Alonso, P. Echenique, F. Falceto, A. Rubio, *J. Chem. Theory Comput.* **2009**, *5*, 728 – 742.
[24] CPMD v3.11.1, Copyright IBM Corp, 1990 – 2008; Copyright MPI für Festkörperforschung Stuttgart, 1997 – 2001; http://www.cpmd.org/.
[25] R. Car, M. Parrinello, *Phys. Rev. Lett.* **1985**, *55*, 2471.
[26] D. Becke, *Phys. Rev. A* **1988**, *38*, 3098.
[27] T. Lee, W. T. Yang, R. G. Parr, *Phys. Rev. B* **1988**, *37*, 785.
[28] O. A. von Lilienfeld, I. Tavernelli, U. Rothlisberger, D. Sebastiani, *Phys. Rev. Lett.* **2004**, *93*, 153004.
[29] O. A. von Lilienfeld, I. Tavernelli, U. Rothlisberger, D. Sebastiani, *Phys. Rev. B* **2005**, *71*, 195119.
[30] T. J. Eisenmayer, H. J. M. de Groot, E. van de Wetering, J. Neugebauer, F. Buda, *J. Phys. Chem. Lett.* **2012**, *3*, 694 – 697.
[31] T. J. Eisenmayer, J. A. Lasave, A. Monti, H. J. M. de Groot, F. Buda, *J. Phys. Chem. B* **2013**, *117*, 11162 – 11168.
[32] S. Hay, N. S. Scrutton, *Nat. Chem.* **2012**, *4*, 161.
[33] G. Kodis, P. A. Liddell, A. L. Moore, T. A. Moore, D. Gust, *J. Phys. Org. Chem.* **2004**, *17*, 724 – 734.
[34] N. Sakai, J. Mareda, E. Vauthey, S. Matile, *Chem. Commun.* **2010**, *46*, 4225 – 4237.
[35] S. V. Bhosale, C. H. Jani, S. J. Langford, *Chem. Soc. Rev.* **2008**, *37*, 331.

Received: June 22, 2014
Published online on September 15, 2014